JOURNAL OF CATALYSIS **117**, 218–236 (1989)

Effects of Preparation, Dispersion, and Extent of Reduction on Activity/Selectivity Properties of Iron/Alumina CO Hydrogenation Catalysts

M. RAMESWARAN AND C. H. BARTHOLOMEW[1]

BYU Catalysis Laboratory, Department of Chemical Engineering, Brigham Young University, Provo, Utah 84602

Received May 30, 1988; revised November 16, 1988

Physical, chemical, and catalytic properties of catalysts prepared by decomposing $Fe(CO)_5$ (carbonyl-derived catalyst, CDC) and $Fe(NO_3)_3$ deposited by aqueous impregnation (conventionally prepared catalyst, CPC) on alumina are compared in this paper. The physical and chemical properties of these catalysts were determined by hydrogen adsorption, oxygen titration, CO temperature-programmed desorption (TPD), and Mössbauer spectroscopy; activity/selectivity properties in CO hydrogenation were determined in a single-pass fixed bed, differential microreactor. Fe/alumina CDCs prepared from γ-alumina dehydroxylated at 923 K are highly reduced, highly dispersed systems. CO-TPD spectra of a CPC and CDCs indicate that the metal crystallites formed on the CPC or on CDCs prepared on poorly dehydroxylated aluminas are probably decorated by support moieties while activity tests indicate them to be less active in CO hydrogenation than CDCs prepared on highly dehydroxylated supports. Furthermore, the activity/selectivity properties of Fe/alumina CDCs do not change with metal dispersion when the extent of reduction is held fairly constant. On the other hand, CO hydrogenation activity of Fe/alumina changes by an order of magnitude with dispersion when changes in *%D* are accompanied by changes in extent of reduction. These results suggest that the "apparent" structure sensitivity observed for CO hydrogenation on iron is probably due to secondary effects such as decoration by support moieties and/or the presence of unreduced metal oxide in the near vicinity of reduced metals.

INTRODUCTION

The influence of surface structure on CO hydrogenation activity and selectivity properties of Group VIII metals (structure sensitivity) is a subject of current interest and has been investigated in a number of previous studies using well-defined single crystals and supported catalysts (*1–11*). While studies of single crystal iron (*12*) and supported iron catalysts (*13*) provide a clear indication of primary structure sensitivity in ammonia synthesis, there are significant discrepancies in the results for single crystal and supported catalyst studies in CO hydrogenation. For example, it is reported (*1, 10, 11*) that structural variations in the crystallite faces of Co, Fe, Ni, and Ru single crystals do not appreciably change CO hydrogenation activity, whereas significant (one to two orders of magnitude) decreases in CO hydrogenation activity with increasing dispersions of supported cobalt, iron, nickel, and ruthenium catalysts are observed (*2–9*). Since the single crystal studies were performed under minimal influence of chemical contaminants and involved at least in one case (*11*) very significant variations in surface structure, they provide strong evidence for the structure insensitivity of these catalysts in CO hydrogenation. The apparent structure insensitivity of these metals in CO hydrogenation is unexpected, since CO adsorbs dissociatively on stepped planes of Co and Ni and on highly strained Co/W(100) but associatively on planer surfaces of Co and Ni (*11, 14–18*).

If not due to structure sensitivity, the activity dispersion trends reported for sup-

---

[1] To whom correspondence should be addressed.

0021-9517/89 $3.00

ported catalysts may be due to secondary effects such as chemical contamination (*19–20*), modification by unreduced oxides (*21–24*), and/or decoration of metal crystallites by support moieties (*25–27*). For example, preferential poisoning of high coordination nickel sites by carbon has been hypothesized by Lee *et al.* (*20*) to explain observed variations in CO hydrogenation activity with dispersion in Ni/alumina and Ni/silica. Preferential decoration of small crystallites by support moieties has been proposed (*23–27*) to explain variations in activity with dispersion of Co and Ni supported on alumina and titania. Metal–metal oxide interactions in alumina-supported cobalt (*24*) and nickel (*22, 23*) systems are thought to be responsible for decreases in activity with decreasing metal loading.

Since it is possible to produce catalysts with high dispersions and high extents of reduction (*28–31*) using carbonyl complexes, carbonyl-derived catalysts (CDCs) are prime candidates for structure sensitivity studies. Furthermore, since CDCs avoid complications due to chemical contaminants such as S, Cl, etc., it is possible to study the reaction free of contaminant effects. Several investigators (*6, 28, 31–33*) have reported that CDCs are 3–50 times more active than catalysts prepared by decomposing inorganic salts onto a support. However, no definitive explanations were given in the literature for their higher CO hydrogenation activity.

Thus, the present study was undertaken to investigate systematically the effects of dispersion, extent of reduction, metal loading, support pretreatment, and preparation method on physical, chemical and catalytic properties of Fe/alumina CO hydrogenation catalysts. The effects of dispersion and extent of reduction on activity/selectivity properties were also simultaneously considered.

EXPERIMENTAL

Catalysts preparation. Previously dried (at 473 K) alumina (DISPAL M, Sample No. 8032 from Conoco) was dehydroxylated under vacuum at 473, 923, and 1073 K for 16 h and stored in a dry box. Approximately a twofold excess of $Fe(CO)_5$ (Stern Chemicals) to achieve a given loading was mixed with pentane. The dehydroxylated alumina was then mixed with this solution and the solvent was removed by evacuation at room temperature. Catalysts thus prepared (CDCs) were sealed in a bottle inside a glove box and stored in a refrigerator at 273 K.

A 4.5% Fe/alumina (conventionally prepared catalyst or CPC) was also prepared by impregnating dried alumina with an aqueous solution of $Fe(NO_3)_3$ to incipient wetness. The wet catalyst was dried in air at 373 K overnight and the nitrate was decomposed by calcining the catalyst at 473 K.

Catalyst reduction. About 1–2 g of catalyst was placed (inside the glove box) in a Pyrex glass flow-through reactor and reduced for 16 h in flowing hydrogen (99.99%, Whitmore) at a space velocity of about 500 h^{-1}. The hydrogen was purified by passing through a Deoxo purifier and a molecular sieve trap. The temperature was raised to the desired reduction temperature at a heating rate of 5 K/min.

Chemisorption measurements. Gas adsorption measurements were performed in a volumetric gas adsorption apparatus described previously (*34*). After reduction the catalyst was evacuated at a few degrees below the reduction temperature to less than 5×10^{-5} Torr for at least 45 min. Since H_2 adsorption on Fe is an activated process (*35*), the sample was exposed at the evacuation temperature to a measured amount of H_2 at 350–450 Torr and cooled to room temperature. The sample was then equilibrated 45 min after which the uptake versus pressure isotherm was measured. Extents of reduction were measured by oxygen titration at 673 K (*36*). Values of metal dispersion (percentage exposed) were calculated from hydrogen uptakes based on the fraction of iron reduced to the metal determined from oxygen uptake values according to calculations in Appendices A and B. It should be emphasized that this approach results in more meaningful and quite different values of dispersion than those based on total iron.

Mössbauer spectroscopy. Mössbauer spectra were obtained using an Austin S-600 spectrometer described previously (*9*). Previously reduced catalyst samples were transferred to a Mössbauer cell in the absence of air or moisture using a Hi Vac glove box. One of the CDCs (4.5% Fe/alumina dehydroxylated at 923 K) which was previously reduced and passivated and the CPC (as prepared) were placed in an *in situ* cell (*9*) for spectral measurements. The passivated CDC was further reduced for only 2 h *in situ*, while the conventional catalyst was reduced *in situ* as described earlier. Spectra were analyzed according to methods reported previously (*9*). Isomer shifts are reported with respect to Fe metal.

CO temperature-programmed desorption (TPD) studies. Approximately 0.05 g of previously reduced and passivated CDC (4.5% Fe/alumina dehydroxylated at 923 K) or CPC was loaded in an all quartz reactor and reduced for 2 or 16 h, respectively. A 10% CO in helium gas was pulsed through the catalysts bed at room temperature until saturation coverage was achieved. The temperature was then increased at 30 K/min while sweeping with ultra high purity He. The desorbing gases were analyzed by a UTI 100C mass spectrometer and the signals were stored in a Sage microcomputer for further analysis. Details of the TPD/mass spectrometer system and analysis were described earlier (*37, 38*).

Activity/selectivity studies. The activity/selectivity measurements were carried out in a single-pass, fixed bed, differential microreactor system described by Rameswaran (*39*). Mixtures of high purity hydrogen and CO ($H_2/CO = 2$ or 3, H_2-Whitmore, 99.99% and CO-Matheson, 99.999%) and H_2 for reduction were further purified using a Pd Deoxo catalyst followed by a Molecular Sieve 5A before admission to the reactor. The product gases were passed through a heated line to a Sigma 1 (Perkin–Elmer) gas chromatograph for on-line analysis. The hydrocarbon products were separated by a 30-m-long, 0.25-mm-diameter fused silica capillary column (Supelco SP-2100) and detected by a flame ionization detector, while the fixed gases were separated by a 6-ft, $\frac{1}{8}$-in.-diameter Chromosorb-102 packed column and detected by a thermal conductivity detector. Activity tests were conducted at three or four different temperatures from which activation energies for CO conversion were calculated. The activity/selectivity data reported in this study were obtained at steady state (after at least 8 h of reaction time). Less than 5% CO conversion was maintained by controlling the reactant flow rate, in order to minimize heat, mass transfer, and pore-diffusional resistances (*40*).

RESULTS

Upon impregnation of dehydroxylated alumina (DHT of 973 K) with $Fe(CO)_5$ the sample was a greenish-brown color; however, after being placed in a sealed bottle for 24 h or more the sample changed to a light brown color. On the other hand, the CDC prepared on the poorly dehydroxylated alumina (dehydroxylation temperature, DHT, of 473 K) turned initially pink. After calcining at 473 K the CPC catalyst was a reddish-orange color.

The extent of reduction to iron metal and percentage metal dispersion (percentage metal exposed) were found to be functions of preparation method, support dehydroxylation temperature, reduction temperature, and metal loading. Relationships among these variables are illustrated in Tables 1 and 2 and in Fig. 1. For example, the effects of reduction temperature on extent of reduction and percentage dispersion (*% D*) at a constant dehydroxylation temperature are depicted for 4.8% Fe–CDC (923 K DHT) in Fig. 1. The extent of reduction increases with increasing reduction temperature to a maximum of 100%, while

TABLE 1

Effects of Metal Loading on the Extent of Reduction and Percentage Dispersion of Fe/Al_2O_3 CDCs Reduced at 573 K

Support dehydroxylation temp.[a] (K)	Wt% Fe[b]	H_2 uptake[c] (μmole/g)	% Reduction[d]	% Dispersion[e]
923	1.0	45.1	67	75
923	1.5	31.5	59	40
923	3.6	55.3	53	33
923	4.5	72.6	55	32

[a] Heated in vacuum at above-mentioned temperature.

[b] Measured by atomic adsorption, after reduction and oxygen titration.

[c] Cooling in 400+ Torr of H_2 from reduction temperature to room temperature.

[d] Measured from O_2 titration.

[e] $\% D$ = (number of surface atoms/total number of reduced atoms) × 100.

TABLE 2

Effects of Support Dehydroxylation Temperature and Preparation Method on the Extent of Reduction and Percentage Dispersion of Fe/Al_2O_3 CDCs and CPC Reduced at 573 K

Cat. type	Support dehydroxylation temp.[a] (K)	Wt% Fe[b]	H_2 uptake[c] (μmole/g)	% Reduction[d]	% Dispersion[e]
CDC	473	4.8	8.9	≤5[g]	50–100[g]
CDC	923	4.5	72.6	55	32
CDC	1073	4.1	55.9	95	16
CPC[f]	473	4.1	12.6	15[h]	24[h]

[a] Heated in vacuum at above-mentioned temperature.

[b] Measured by atomic adsorption, after reduction and oxygen titration.

[c] Cooling in 400+ Torr of H_2 from reduction temperature to room temperature.

[d] Measured from O_2 titration at 673 K; unless otherwise noted calculated according to Appendix A.

[e] $\% D$ = (number of surface atoms/total number of reduced atoms) × 100 = $1.117X/(Wf)$, where X = H_2 uptake (μmole/g), W = wt% Fe, and f = fraction of iron reduced to metal (*9*).

[f] Prepared by $Fe(NO_3)_3$ aqueous impregnation.

[g] Estimated from Mössbauer spectrum of reduced catalyst.

[h] Average of values from Appendices A and B.

the $\% D$ goes through a maximum (29%) at 573 K. Hence a reduction temperature of 573 K was used for reducing the remaining catalysts in this study. The data in Table 1 show that at a constant DHT of 923 K the extent of reduction is reasonably constant (53–67%) while $\% D$ decreases with increasing metal loading.

From the results in Table 2 it is evident that dispersions of CDCs (metal loading held constant) decrease with increasing dehydroxylation temperature, whereas extents of reduction increase with increasing dehydroxylation temperature. In fact 95% reduction was achieved for a 4.1% Fe–CDC (1023 K DHT) at a reduction temperature as low as 573 K. Several investigators (*40–43*) have reported very low extents of reduction (1–10%) for 1–4% Fe/Al_2O_3 CPCs even at much higher reduction temperatures than in this study.

Mössbauer spectra and parameters of an unreduced, vacuum-dried 4.5% Fe–CDC (923 K DHT) and the air-dried CPC are compared in Fig. 2 and Table 3. Although the isomer shifts are the same within experimental error, the difference in quadrupole splittings is significant.

The Mössbauer spectra of reduced CDCs (dehydroxylated at different temperatures) and the CPC are shown in Fig. 3. Table 4 lists the parameters obtained by curve fitting spectra in Fig. 3. Curve fits of the spec-

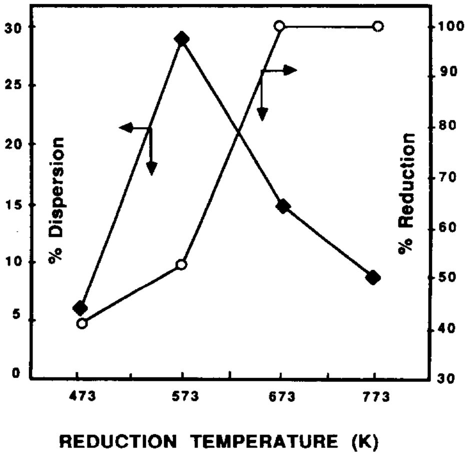

FIG. 1. Effects of reduction temperature on $\% D$ and extent of reduction for 4.8% Fe–CDC (alumina dehydroxylated at 923 K).

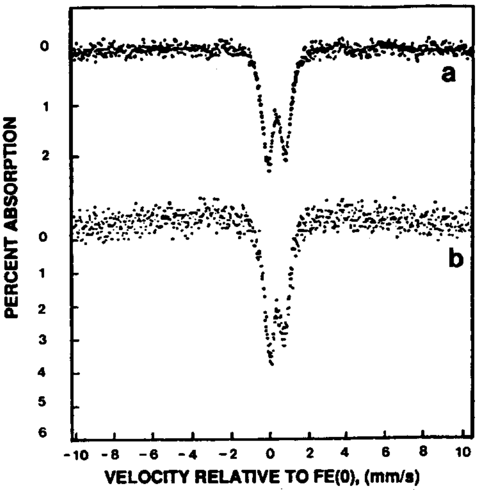

FIG. 2. Mössbauer spectra of unreduced, dried (a) CDC and (b) CPC samples.

tra for the CPC and CDC (473 K DHT) are consistent with the presence of small amounts (5–16%) of paramagnetic forms of Fe^0 while ferromagnetic iron is clearly present in CDC catalysts for which the support was dehydroxylated at 923 and 1073 K. The trend of increasing extent of reduction with increasing dehydroxylation temperature (Figs. 3b–3d and Table 4) is in good qualitative agreement with that obtained by H_2 chemisorption and O_2 titration, as tabulated in Table 2. The isomer shifts and hyperfine fields of the Fe^0 sextets for Fe–CDCs (923 and 1023 K DHT) are almost identical to that of pure Fe foil (Table 4).

Figures 4 and 5 show the TPD spectra for CO and CO_2 on the CPC and 4.5% Fe–CDC (923 K DHT), respectively. Figure 5 shows spectra for two different samples of the same catalyst (4.5 Fe–CDC, 923 K DHT); the right spectrum includes data collected at a higher temperature range. It is evident in comparing Figs. 4 and 5 that a highly populated, high temperature CO binding state for the CPC is observed at about 750 K while two such states are observed for the CDC at about 700 and 873 K. Nevertheless, a lowly populated, low temperature CO state at 373 K is observed for both catalysts. The CO_2 desorption peak is observed at a lower temperature for the CPC relative to the CDC.

CO turnover frequencies (TOFs) and rates of CO conversion (per gram of catalyst) for CO hydrogenation on Fe/alumina CDCs of different loadings (support dehy-

TABLE 3

Mössbauer Parameters for Unreduced, Dried Samples of Fe/Al_2O_3–CPC and CDC

Species	Isomer shift[a] (mm/s)	Quadrupole splitting (mm/s)	Hyperfine field (kOe)	% Area
4.5% Fe–CDC, support dehydroxylated at 923 K				
$Fe(CO)_x$ (x = 3, 4) or $Fe_3(CO)_y$ (y = 9, 10)	0.36	0.95	—	100
4.1% Fe-conventional catalyst (CPC)				
Fe^{3+}	0.35	0.77	—	100

[a] Relative to Fe^0.

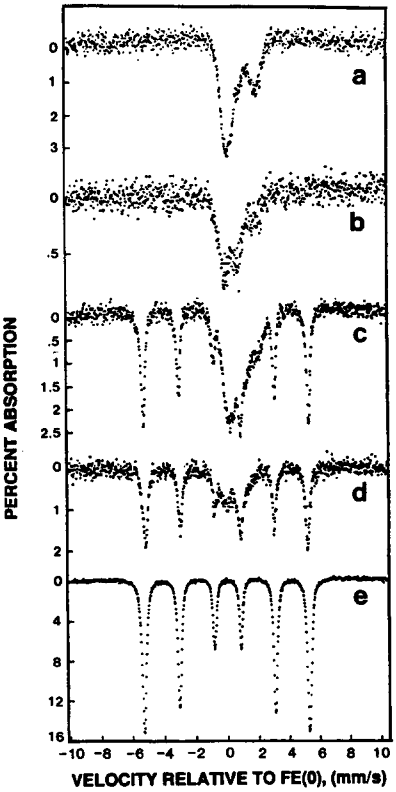

FIG. 3. Mössbauer spectra of reduced catalysts. (a) CPC, (b–d) 4.5% CDCs (473, 923, and 1073 K DHT), and (e) Fe foil standard.

TABLE 4

Mössbauer Parameters for Reduced[a] ~4.5% Fe/Al_2O_3 Dehydroxylated at Varying Temperatures

Species	Isomer shift[b] (mm/s)	Quadrupole splitting (mm/s)	Hyperfine field (kOe)	% Area
	Conventional catalyst (CPC)			
Fe^0	−0.05	—	—[c]	16
Fe^{2+}	1.38	1.36	—	64
Fe^{3+}	0.30	0.59	—	20
	CDC, 473 K dehydroxylation			
Fe^0	−0.05	—	—[c]	5
Fe^{2+}	1.12	1.79	—	34
Fe^{3+}	0.38	0.93	—	61
	CDC, 923 K dehydroxylation			
Fe^0	0.01	—	327	36
Fe^{2+}	1.0	1.8	—	10
Fe^{3+}	0.44	1.04	—	54
	CDC, 1073 K dehydroxylation			
Fe^0	0.01	—	334	68
Fe^{3+}	0.35	1.02	—	36
	Iron foil			
Fe^0	0.01	—	328	100

[a] Reduction temperature of 573 K.
[b] Relative to Fe^0.
[c] Superparamagnetic Fe singlet.

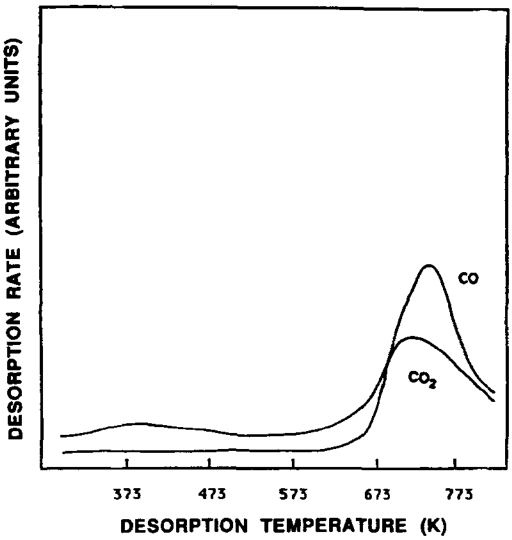

FIG. 4. CO- and CO_2-TPD spectra for the CPC.

droxylated at 973 K) are listed in Table 5. The activation energies for CO conversion (E_{CO}) were calculated from an Arrhenius plot of TOFs at three or more temperatures. The following observations can be

TABLE 5

Effect of Metal Loading on CO Hydrogenation Activity of Fe/Al_2O_3 CDCs, Support Dehydroxylated at 973 K (H_2/CO = 2, 1 atm), Reduced at 573 K

Wt% metal	Reaction temp. (K)	% CO conversion	$N_{CO} \times 10^3$ [a] (s^{-1})	Rate × 10^6 [b] (mole g^{-1} m^{-1})	E_{CO}[c] (kJ/mole)
1.0	473	0.59	0.12	0.66	75 ± 7
% D = 75	488	0.77	0.26	1.40	
% R = 67	498	0.80	0.32	1.75	
	513	1.18	0.55	2.98	
1.5	473	0.45	0.13	0.49	72 ± 1
% D = 40	488	0.37	0.23	0.87	
% R = 59	498	0.40	0.32	1.22	
	513	0.66	0.54	2.03	
3.6	488	0.83	0.23	1.54	71 ± 1
% D = 33	498	1.26	0.33	2.21	
% R = 53	513	1.01	0.54	3.58	
4.5	488	0.60	0.21	1.84	85 ± 8
% D = 32	498	0.97	0.35	3.04	
% R = 55	513	1.71	0.59	5.18	

[a] N_{CO}, molecules of CO converted per exposed site second.
[b] Rate, moles of CO converted per gram of catalyst minute.
[c] Activation energy for CO conversion.

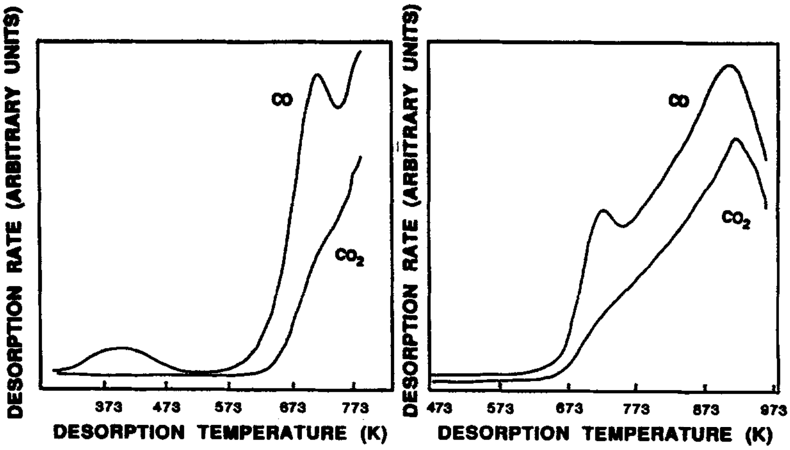

FIG. 5. CO- and CO_2-TPD spectra for the 4.5% Fe–CDC (923 K DHT).

made from the data in this table: (i) TOFs do not change appreciably with metal loading (or with percentage dispersion) although rates (per gram) increase as expected with increasing metal loadings and (ii) values of E_{CO} do not change very much with metal loading (or with percentage dispersion). Similarly, no significant differences in selectivity properties were found for these catalysts (see Table 6); olefin/paraffin ratios were observed in the range of 1–3.5 while Anderson–Schulz–Flory plots were found to be linear from which α values in the range 0.52–0.63 were calculated.

TABLE 6

Effect of Metal Loading on CO Hydrogenation Selectivity of Fe/Al_2O_3 CDCs Having the Support Dehydroxylated at 923 K (H_2/CO = 2, 1 atm), Reduced at 573 K

Wt% Fe	Temp. (K)	% CO conversion	% HC product[a]	Selectivity[b]				O/P[c]	α[d]
				CH_4	C_2–C_4	C_5–C_{11}	C_{12+}		
1.0	473	0.59	67	24	42	34	0	1.7	0.56
	488	0.77	76	25	44	30	2	1.5	0.58
	498	0.80	73	27	41	32	0	2.0	0.57
	513	1.18	74	32	46	22	0	1.8	0.52
1.5	473	0.45	80	28	43	29	0	2.5	0.55
	488	0.37	68	26	43	31	0.4	2.5	0.57
	498	0.40	85	24	47	29	0	2.3	0.57
	513	0.66	82	29	45	25	0.5	2.5	0.56
3.6	488	0.83	88	20	37	41	2	0.9	0.63
	498	1.26	86	21	40	35	3	2.3	0.61
	513	1.01	82	27	45	26	0.8	3.5	—
4.5	488	0.60	90	22	40	35	3	1.7	0.63
	498	0.97	79	22	40	37	2	1.7	0.66
	513	1.71	83	23	45	30	2	1.7	0.59

[a] At% HC = (hydrocarbon) × 100/(hydrocarbon + CO_2), based on carbon balance.

[b] Hydrocarbon selectivity (wt%) based on 100% HC.

[c] $O/P = \Sigma_3^7 C_n^{2-}/\Sigma_3^7 C_n$.

[d] Anderson–Schulz–Flory chain propagation probability.

TABLE 7

Effects of Dehydroxylation Temperature and Method of Preparation on the Activity of 4–5% Fe/Al_2O_3 Catalysts ($H_2/CO = 2$, 1 atm), Reduced at 573 K

Dehydroxylation temp. (K)	Reaction temp. (K)	% CO conversion	$N_{CO} \times 10^3$ [a] (s^{-1})	Rate $\times 10^6$ [b] (mole g^{-1} m^{-1})	E_{CO}[c] (kJ/mole)
473	473	0.05	0.04	0.04	38 ± 12
CDC	488	0.06	0.05	0.05	
(4.8% Fe)	498	0.07	0.05	0.06	
	513	0.11	0.09	0.09	
923	488	0.60	0.21	1.84	85 ± 8
CDC	498	0.97	0.35	3.04	
(4.5% Fe)	513	1.71	0.59	5.18	
1073	473	0.52	0.04	0.26	191 ± 21
CDC	488	1.28	0.17	1.11	
(4.1% Fe)	498	2.49	0.64	4.28	
	513	4.81	1.79	12.0	
CPC	488	0.18	0.12	0.18	75 ± 3
(4.1% Fe)	498	0.25	0.17	0.26	
	513	0.44	0.30	0.46	

[a] N_{CO}, molecules of CO converted per exposed site per second.

[b] Rate, moles of CO converted gram of catalysts per minute.

[c] Activation energy for CO conversion.

TABLE 8

Effects of Dehydroxylation Temperature and Method of Preparation on the Selectivity of 4–5% Fe/Al_2O_3 Catalysts ($H_2/CO = 2$, 1 atm), Reduced at 573 K

Dehydroxylation temp. (K)	Temp. (K)	% CO conversion	% HC in product[a]	Selectivity[b]				O/P[c]	α[d]
				CH_4	C_2–C_4	C_5–C_{11}	C_{12+}		
473	473	0.05	23	43	56[e]	0	0	1.5	—
CDC	488	0.06	30	43	57[f]	0	0	2.2	—
	498	0.07	61	36	57	7	0	0.8	—
	513	0.11	44	41	48	11	0	1.1	—
923	488	0.60	90	22	40	35	3	1.7	0.63
CDC	498	0.97	79	22	40	37	2	1.7	0.66
	513	1.71	83	23	45	30	2	1.7	0.59
1073	473	0.52	68	24	38	38	0	2.7	0.61
CDC	488	1.28	90	19	38	43	0	1.5	0.64
	498	2.49	93	16	39	41	4	1.5	0.64
	513	4.81	89	16	41	41	2	1.2	0.62
CPC	488	0.18	51	23	42	35	0	3.2	—
	498	0.25	65	20	40	40	0	3.1	—
	513	0.44	72	24	42	34	0	2.6	—

[a] At% HC = (hydrocarbon) × 100/(hydrocarbon + CO_2), based on carbon balance.

[b] Hydrocarbon selectivity (wt%) based on 100% HC.

[c] $O/P = \Sigma_3^7 C_n^{2-}/\Sigma_3^7 C_n$.

[d] Anderson–Schulz–Flory chain propagation probability.

[e] C_2 and C_3 only.

[f] C_2, C_3, and C_4 only.

Tables 7 and 8 compare the CO hydrogenation activity/selectivity properties of CDCs prepared by dehydroxylating the support at varying temperatures with those of the CPC. Interestingly, the TOF (at all temperatures except 488 K), E_{CO}, and selectivity for C_{5+} hydrocarbons of CDCs increase with increasing dehydroxylation temperature while the selectivity for methane decreases. The CPC is more active than the Fe–CDC (473 K DHT). However, at any given temperature the other CDCs (923 or 1023 K DHT) are a factor of 3–10 times more active than the CPC. The hydrocarbon selectivities of the poorly reduced CDC (473 DHT) and the CPC are 20–50% lower relative to well-reduced CDCs (compare Tables 6 and 8). The olefin/paraffin (C_3–C_7) ratios of the CPC are about the same or only slightly (1.5–2 times) higher than those of the CDCs.

DISCUSSION

CHEMICAL, PHYSICAL, AND CATALYTIC PROPERTIES OF Fe/ALUMINA CDCs AND THEIR BEHAVIOR RELATIVE TO Fe/ALUMINA CPCs

Chemical and Physical Properties of Fe/Alumina (CDCs and CPCs)

Catalyst precursors. The greenish-brown color of CDCs on dehydroxylated supports is characteristic of physically adsorbed $Fe(CO)_5$ (*28*a, *44*) and $Fe_3(CO)_{12}$ from photochemically induced surface reaction of $Fe(CO)_5$ (*45*), while the change to light brown upon standing is probably due to partial decarbonylation due to chemisorption on the dehydroxylated alumina (*28*a). The pink color of the poorly dehydroxylated (at 473 K) CDC catalyst is likely due to formation of $[HFe(CO)_4]^-$ or $[Fe(CO)_4]^{2-}$ as a result of partial decarbonylation and oxidation by hydroxyl groups (*46–48*). The reddish-brown color of the calcined (at 473 K) CPC and its Mössbauer parameters are characteristic of well-dispersed α-Fe_2O_3 (*49, 50*) or Fe^{III}/alumina (*48, 51, 52*) while the green–brown colors of the freshly impregnated, dried CDC catalysts (DHT of 923 K) are consistent with adsorbed subcarbonyls of iron, $Fe(CO)_x$ (x = 3 or 4) and $Fe_3(CO)_y$ (y = 9–10) (*28, 44*). The Mössbauer spectrum for the dried, unreduced Fe/alumina CDC (Table 3) is characteristic of adsorbed $Fe_3(CO)_y$ (y = 9–10) (*44*).

Reduced catalysts. The results of this study show that dilute Fe/alumina catalysts prepared from decomposition of carbonyls on highly dehydroxylated alumina (CDCs, DHT of 923 K) and reduced at a moderate temperature (573 K) in hydrogen have significantly higher dispersions (32–75%) and substantially higher extents of reduction to the metal (55–67%) than those (%D = 24%; %R = 15%) for 4.1% Fe/alumina prepared by conventional impregnation (CPC). The extent of reduction for base/metal alumina CPCs is generally found to be a function of metal loading (*2, 4, 5, 36*). Moreover, the extent of reduction of base metals on alumina at low loadings (1–3%) is generally quite low (5–20%) (*2, 5, 32, 36, 43*). Indeed, it is observed (*32, 43*) that up to 300 μmole (~1.6 wt%) of Fe on alumina (CPC) is rendered irreducible even at very high reduction temperatures due to the influence of the support. Thus, the low extent of reduction (15%) observed for the 4.1% Fe/alumina in this study is consistent with this previous experience. Moreover, the results of this study (Table 1) indicating that the extent of reduction of Fe/alumina CDCs (923 K DHT) is high (above 50%) and fairly constant with metal loading are consistent with the previous work with these catalysts (*28–31*). The observation in this study that the extent of reduction increases with increasing support dehydroxylation temperature (or decreasing concentration of surface hydroxyl groups, σ-OH) is a new result but consistent with principles reported previously (*28, 29, 53–56*). Several researchers (*28, 29, 53–56*) have reported that the σ-OH groups on the alumina surface act as anchors for carbonyls by partially oxidizing them. Thus, as the concentration of σ-OH groups decreases on the surface of a support the extent of oxidation also should decrease (and extent of reduction increase).

It should be emphasized that the determination of extent of reduction in Fe/alumina catalysts is not trivial because of the multiplicity of oxidation states (Fe^0, Fe^{II}, and Fe^{III}) and phases (Fe^0 paramagnetic, Fe^0 ferromagnetic, $FeAl_2O_4$, Fe_3O_4, and Fe_2O_3) present in the reduced forms of these catalysts. Accordingly, a discussion of the methods used to estimate the extent of reduction is appropriate here.

The extents of reduction calculated from oxygen titration (OT) and from Mössbauer spectroscopy for CDCs and CPC agree well within reasonable limits (see Tables 2 and 4). The following assumptions were made in calculating extents of reduction from OT for highly dehydroxylated CDCs: (i) After reduction, most or all of the unreduced iron is present in the form of a stable Fe^{III} oxide or oxyhydroxide (*44, 48, 51, 52*) interacting strongly with alumina, (ii) during the oxygen titration at 723 K all of the Fe^0 converts to Fe_2O_3 or similar Fe^{III} oxide in the presence of oxygen, and (iii) the amount of O_2 consumed by Fe^{2+}, if any, is either negligible or Fe^{2+} is present in a very stable form such as $FeAl_2O_4$ and thus is not oxidized back to Fe^{3+}. These assumptions are consistent with those in Appendix A; accordingly, the OT stoichiometry and calculations in Appendix A apply.

Assumptions (i) and (iii) are supported by the Mössbauer analysis for reduced CPCs dehydroxylated at higher temperatures DHT of 923 and 1023 K (See Table 4) showing mostly Fe^0 and Fe^{3+} to be present in the sample. They are further consistent with reactions reported by Brenner and Hucul (*28*a) for high temperature decomposition of $Fe(CO)_3$ (ads) on partially dehydroxylated (PDA) alumina:

$$Fe(CO)_3/PDA \rightarrow Fe/PDA + 3\ CO \quad (1)$$

$$Fe(CO)_3/PDA + 2\ \sigma{-}OH \rightarrow Fe^{III}OOH + \tfrac{1}{2}\ H_2 + 3\ CO \quad (2)$$

Assumption (ii) is consistent with Mössbauer data from previous studies (*48, 51, 52*) showing that well-dispersed alumina-supported Fe^0 is oxidized to mainly Fe_2O_3 or other similar Fe^{III} oxides during air exposure at modest temperatures (298 K and above).

However, these assumptions are apparently not valid for Fe/alumina catalysts prepared by aqueous impregnation (CPC) or by carbonyl decomposition on supports dehydroxylated at low temperature (e.g., DHT of 473 K). Indeed the Mössbauer spectra for the reduced CPC and CDC (DHT of 473 K) (Table 4) indicate the presence of large fractions of Fe^{2+} and relatively small quantities of superparamagnetic $Fe^{(0)}$. Accordingly a different set of assumptions which account for the oxidation of Fe^{II} species during the OT may be appropriate. Assuming that the Fe^{II} species in Fe_3O_4 is oxidized to Fe_2O_3 (consistent with the observation in the calcined catalyst of a reddish-brown material) and utilizing the information from the hydrogen adsorption and OT along with Fe^{2+}/Fe^{3+} ratio from the Mössbauer spectrum, the minimum concentration of Fe^0, the corresponding extent of reduction, and $\% D$ are estimated for the CPC (see Appendix B) to be 59 μmole/g of catalyst, 8.1%, and 43%, respectively. Assuming the Fe^{II} in the CPC is not oxidized during titration, the maximum concentration of Fe^0, extent of reduction, and dispersion are estimated (Appendix A) to be 120 ($\frac{4}{3} \times 90$) μmole/g, 17%, and 21%, respectively; therefore, the true extent of reduction for the reduced CPC should be between 8.1 and 17%. The average of these two values (12%) was chosen for Table 2 because in fact some but not all of the Fe^{II} species are oxidized to Fe_2O_3 during titration (*52*).

The observation of superparamagnetic Fe^0 in the CPC and CDC (DHT of 473 K) is consistent with a previous Mössbauer study of 1% Fe^{57}/alumina CPC (*52*). Superparamagnetic Fe^0 has also been observed in the Fe/carbon system (*9*) and is attributed to either strong Fe–carbon interaction or the presence of carbon contaminants on the iron metal surface. The fact that superparamagnetic Fe^0 is observed in the CPC and the CDC prepared from poorly dehydroxylated alumina while ferromagnetic Fe^0 is observed in the CDCs prepared from the two highly dehydroxylated aluminas (Table 4) is significant. It suggests that the iron clusters in the former two catalysts may be perturbed (e.g., decorated with support or iron oxide material). On the other hand, the very good agreement of Mössbauer parameters for the latter two catalysts with those of the Fe foil suggests that the relatively small iron cystallites are not perturbed by foreign material and thus exhibit collective magnetism or ferromagnetism.

While decoration of metal crystallites by reduced support species which migrate during reduction on to the surface is well-documented in metal/titania systems (*25*, *26*, *58*), the decoration of metal crystallites by alumina species must occur by some other mechanism since alumina is not reducible at typical reduction temperatures. Wheeler and Bettman (*57*) demonstrated that the hot acidic liquid formed during calcination of nitrate impregnated catalysts dissolves some of the alumina and dopes the metal oxide with support material during calcination. Since the CPC of this study was prepared from the iron nitrate, it is possible that the iron oxide in the CPC was similarly doped with alumina prior to the reduction leading to "decorated" metal particles after reduction (see Fig. 6a).

Since neither the metal nor the support is exposed to an acidic environment in the preparation of highly dehydroxylated CDCs, the surface of the metal crystallites on CDCs should, in principle, remain "clean" during preparation (see Reaction 1 and Fig. 6b). Moreover, the preparation of clean crystallites is also more likely for CDCs of high DHT because the catalyst activation involves decarbonylation of subcarbonyls and/or mild reduction of nonspinel oxyhydroxide species (see Reaction 2) while the reduction of the conventional catalyst or CDC of low DHT could lead to decoration via decomposition of the spinel (*27*).

The TPD data presented earlier (Fig. 4 and 5) provide further evidence that the CPC is decorated. Indeed, the most important difference between the TPD spectra of the CPC and CDC (Figs. 4 and 5) is the difference in the position of the major CO desorption peaks. These spectra indicate that the binding energy for CO is significantly lower for the CPC than for the CDC. Raupp and Dumesic (*25*) observed from TPD spectra that decorating a clean Ni foil with alumina decreases the CO binding energy. Moreover, Bartholomew *et al.* (*58*, *59*) observed high temperature activated states for hydrogen adsorption on Ni/alumina nearly identical to those observed by Raupp and Dumesic (*25*) for an alumina-decorated nickel film. Accordingly the results of this study, together with these previous investigations (*25*, *27*, *58*, *59*), provide strong evidence that alumina decorants are present in alumina-supported base metal CPCs which increase the binding energy of hydrogen while decreasing that of CO.

Reaction-aged catalysts. The results of this study do not provide direct information on the chemical and physical properties of the catalysts during or after reaction in synthesis gas. However, a recent previous investigation in this laboratory of dilute Fe/alumina (*52*) and several recent investigations of Fe/alumina (*60–62*) by Mössbauer spectroscopy provide some insights. For example, studies of 10% CPCs (*60*, *61*) and a 14% CDC (*62*) indicate that (i) reduction at 673 K transforms about 70% of the iron to ferromagnetic iron and (ii) reaction at 525–550 K in synthesis gas results in carbiding of essentially all of the ferromagnetic iron, while the unreduced iron is unaffected. On the other hand, reduction of 1–3% Fe/alumina CPC catalysts at 673–773 K transforms only 10–20% of the iron to superparamagnetic clusters, while reaction at 493–513 K causes little change in either these clusters or the oxide phases (*52*). Ac-

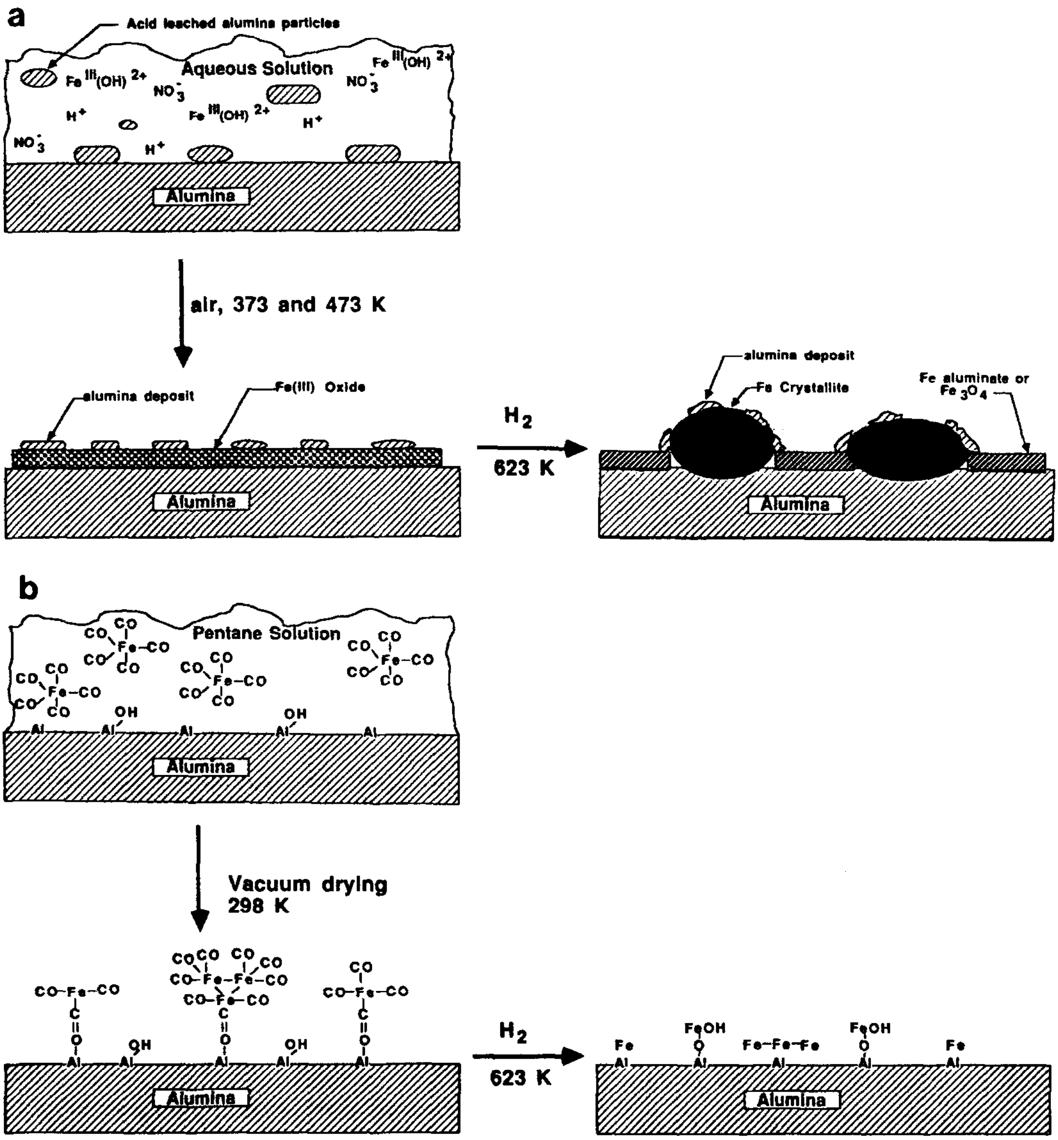

FIG. 6. Models for preparation of (a) CPC and (b) CDC catalysts.

cordingly, it would be expected that the ferromagnetic iron phases in the catalysts of this study would have been transformed to carbides during reaction, while superparamagnetic iron and iron oxide phases would have remained uncarbided.

Catalytic Properties of Fe/Alumina CDCs and CPCs

CO hydrogenation activity. While activity data were previously reported for Fe/alumina CDCs (*28*c, *30–32*, *63–66*) and CPCs (*32*, *67*) there are apparently large discrepancies in the values where comparison is possible. Some of the data cannot be easily compared quantitatively because (i) catalyst surface areas were not reported and/or (ii) attention was not given to important parameters that affect activity such as dehydroxylation temperature. Nevertheless, it is possible to estimate a lower bound on turnover frequency, i.e., formal turn-

TABLE 9

Comparison of Specific Activities for CO Hydrogenation on Fe/Al_2O_3 CDC and CPC Catalysts at 523 K, H_2/CO = 2

Wt% Fe	Precursor	DHT[a] (K)	Temp. tested (K)	% CO conversion	TOF[b] × 10^3	$(TOF)_f$[c] × 10^3	Reference
0.82	$Fe_3(CO)_{12}$	298	543	3.3	—	0.053	(*63, 65*)
1.85	$Fe(CO)_5$	298	533	3.3	—	0.043	(*63, 65*)
4.8	$Fe(CO)_5$	473	513	0.11	0.13	0.10	This study
1.73	$Fe_3(CO)_{12}$	873	523	0.06	—	1.6	(*66*)
1.5	$Fe_3(CO)_{12}$	973	525	8.8	2.5	1.8	(*31*)
2.6	$Fe_3(CO)_{12}$	923	525	6.5	1.9	0.50	(*31*)
~2	$[Et_4N][HFe_3(CO)_{11}]$	923	525	4.6	0.9	0.23	(*31*)
1.5	$Fe(CO)_5$	973	513	0.66	0.75	0.56	This study
4.5	$Fe(CO)_5$	973	513	1.71	0.86	0.28	This study
4.1	$Fe(CO)_5$	1073	513	4.8	4.2	0.67	This study
4.1	$Fe(NO_3)_3$	Aq. Impreg.	513	0.44	0.42	0.13	This study
15	$Fe(NO_3)_3$	Aq. Impreg.	523	—	0.63	0.047	(*67*)

[a] Dehydroxylation temperature of alumina support.

[b] Turnover frequency for CO conversion in CO molecules converted per catalytic site per second.

[c] Formal CO turnover frequency in CO molecules converted per iron atom per second (based on total iron atoms in sample). $(TOF)_f = D(TOF)$ where D = dispersion or percentage exposed (*28c*).

over frequency (*28*c), by assuming these catalysts were completely dispersed—an assumption very probably valid to within a factor of 2 or 3 based on the data from this and previous studies showing CDCs to have dispersions in the range of 30–70%. Moreover, what is very significant, this study provides the basis for explaining the apparent discrepancies in the previously reported activity data. Accordingly previously reported data are compared with the results of this study in Table 9.

The data in Table 9 show that CDCs prepared on alumina supports dehydroxylated above 873 K are in the same range of activity (0.8 to 4 × 10^{-3} s^{-1}), 5–10 times more active than catalysts prepared on aluminas evacuated or dried at 298–473 K and 2–10 times more active than CPCs. In several previous studies (*28, 30–33*) CDCs were also observed to have higher activities for CO hydrogenation and other reactions than their counterparts prepared by conventional aqueous techniques. This observation of significantly higher activity for the CDCs of high DHT is consistent with the earlier stated hypothesis of a clean metal surface for these catalysts while surfaces are thought to be decorated with support contaminants in the catalysts prepared on supports having high concentrations of hydroxyl groups. This hypothesis is also consistent with recently reported TPD/TPSR data (*38, 68*) indicating that a 1% Co/alumina CPC which does not adsorb CO dissociatively (rather only weakly and molecularly) is inactive for CO hydrogenation, while 3, 10, and 15% Co/alumina catalysts which adsorb CO progressively more strongly are progressively more active in that order; these results have been interpreted in terms of a support decoration and intimate interaction of metal clusters with metal oxide phases, the effects of which are progressively greater in low loading catalysts having smaller metal crystallites (*38, 68*).

Chen *et al.* (*33*) attributed the higher activity of CDCs to their ability to adsorb hydrogen more competitively. While from a kinetics consideration a higher hydrogen coverage would lead to higher activity, these authors did not explain why hydrogen would be more strongly held on CDCs. In fact, the results of this study coupled with those of Raupp and Dumesic (*25*) indicate that CDCs bind hydrogen less strongly and CO more strongly than CPCs, the latter probably involving decoration of the metal surface by support species. Accordingly, a more reasonable explanation for the higher activities of alumina-supported CDCs is the ability of their clean surfaces to dissociate CO more readily, since at low reaction temperatures the rate-determining step (or co-rate-determining step) in CO hydrogenation may be CO dissociation (*26*). Moreover, it is possible that CPC catalysts may bind hydrogen too strongly; that is, the high binding energy coupled with the presence of surface contaminants may limit the mobility of hydrogen and its access to carbon containing intermediates (*26, 69*).

CO hydrogenation selectivity. Hughes *et al.* (*64*) reported unexpectedly high olefin (especially propylene) selectivities for CO hydrogenation on a Fe/alumina CDC catalyst prepared on alumina dehydroxylated at 298 K. This observation together with a few similar observations for other Fischer–Tropsch CDCs has sparked the hope that cluster catalysts could be developed having high olefin selectivities (*28*c). However, the selectivity data of this study which resulted from a very careful analysis of the reaction products at steady state (after 24 h of reaction) indicate that the selectivity properties of Fe/alumina CDCs prepared on highly dehydroxylated alumina are not markedly different than those observed for conventional iron Fischer–Tropsch catalysts. In fact the broad hydrocarbon product distributions are those predicted by the Anderson–Schulz–Flory polymerization model (*70*). Moreover, the olefin/paraffin ratios of these catalysts of 1–3 are not unusual for unpromoted iron catalysts (*69, 70*). The only significant difference is that CO_2 selectivity is clearly lower (% HC is higher) for CDCs relative to CPCs or poorly reduced CDCs (Tables 6 and 8). Accordingly the unusual olefin selectivities observed by Hughes et al. (*64*) are not representative of catalysts prepared from carbonyl clusters and may have resulted from (i) an experimental artifact of not having reached steady state or (ii) may be explained by unusual promotional effects of Fe oxide or support decorants in poorly reduced catalysts that typically result from preparation on a poorly dehydroxylated support (*28*, Table 2). Rankin and Bartholomew (*69*) likewise observed unusually high olefin selectivities for Fe/silica and Fe/K/silica catalysts that had been precalcined at 473 K which they attributed to a promotional effect of iron silicates or iron potassium silicates on the iron surface which significantly increase the binding energy of hydrogen while decreasing its rate of adsorption/desorption thereby limiting the access of carbon-containing intermediates to hydrogen during reaction. Unfortunately, in both of these studies the high olefin selectivities (*64, 69*) were associated with Fischer–Tropsch activities two or three orders of magnitude lower than observed for commercial FT catalysts (*70*).

EFFECTS OF DISPERSION AND EXTENT OF REDUCTION ON THE ACTIVITY/SELECTIVITY PROPERTIES OF Fe/ALUMINA: STRUCTURE-SENSITIVITY OR PROMOTER/SUPPORT EFFECTS?

As pointed out under the Introduction there is a discrepancy between the results obtained for single crystal metals in CO hydrogenation (*1, 10, 11*) indicating no significant change in activity with structure and those for supported metals indicating one to two orders of magnitude change in activity with changes in dispersion (*2–9*). However, in these supported catalyst studies variations in dispersion were generally accompanied by variations in metal loading and extent of reduction (although, Bell and Kellner (*3*) and Jung *et al.* (*8*) did not report extents of reduction for their catalysts). Thus, it is possible that the "apparent" structure sensitivity of supported Fe, Ni, and Ru catalysts is caused by secondary

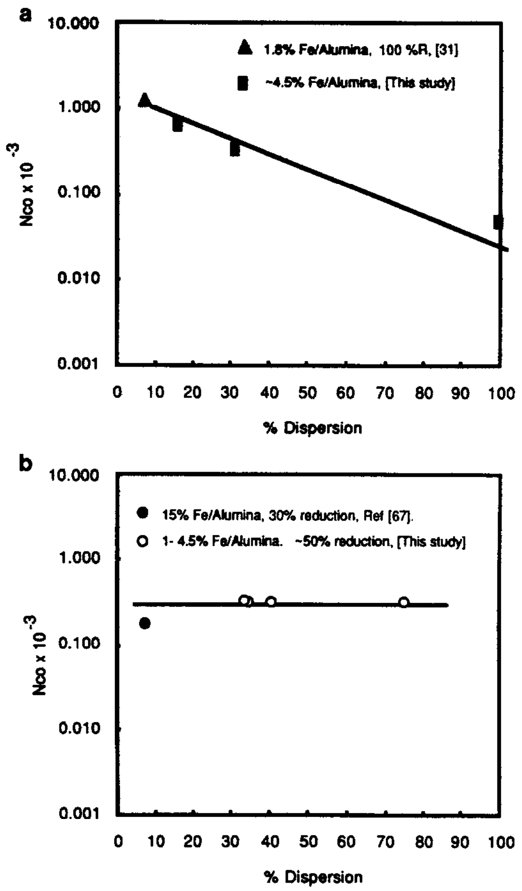

FIG. 7. (a) Activity of Fe/alumina as a function of dispersion with varying extent of reduction (% *R*). (b) Activity of Fe/alumina as a function of dispersion with constant % *R*.

effects such as the presence of unreduced metals or support effects, e.g., support decoration.

Indeed, an order of magnitude change in CO hydrogenation activity with increasing dispersion is observed for the carbonyl-derived catalysts of this and a previous study (*31*) for which extent of reduction was varied over a wide range (see Fig. 7a). Moreover, Fig. 8 shows that the activities of Fe/alumina, Fe/magnesia, and Fe/carbon catalysts reported in this and previous studies (*7, 9, 31, 67*) increase by about an order of magnitude with increasing extent of reduction. Most significantly, the data in Fig. 7b from this and a previous study (*67*) indicate that *the activity of Fe/alumina remains constant when dispersion is changed while the extent of reduction is held reasonably constant* (ca. ±20%). Thus, Figs. 7 and 8 show that changes in the extent of reduction account for the observed changes in activity with dispersion; accordingly, *the results of this study together with those from previous studies provide strong evidence that the CO hydrogenation reaction is structure insensitive on supported Fe catalysts*. While the available data do not provide a conclusive basis for separating the contributions of two different effects, e.g., iron oxide modification and support decoration, the threefold higher activity for unsupported iron relative to 100% reduced Fe/alumina (Fig. 8) in this case favors the hypothesis of support decoration, i.e., it might be difficult to completely eliminate support decoration even in highly reduced Fe/alumina catalysts, whereas effects of iron oxide modification would clearly be absent at 100% reduction.

CONCLUSIONS

1. Dilute Fe/alumina catalysts prepared from decomposition of carbonyls (CDCs) on highly dehydroxylated alumina and reduced at a moderate temperature (573 K) in hydrogen have significantly higher dispersions (32–75%) and substantially higher extents of reduction to the metal (55–67%) than those (% $D \leq 24\%$; % $R \leq 15\%$) for dilute Fe/alumina catalysts prepared by conventional aqueous impregnation methods (CPCs). The extent of reduction increases while dispersion decreases for CDCs with increasing dehydroxylation temperature of the alumina support.

2. Modifications in the magnetic properties of metallic iron observed by Mössbauer Spectroscopy and in the TPD spectrum for CO adsorption on Fe/alumina catalysts of low reduction (CPC and CDC prepared on alumina dehydroxylated at 473 K) may result from decoration of the metal by either support moieties or iron oxide phases formed during preparation. These effects are apparently absent in the Mössbauer and TPD spectra for CDC catalysts prepared on

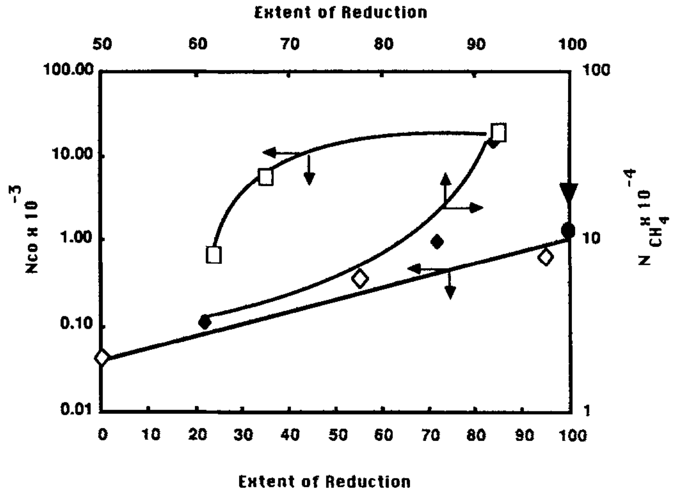

FIG. 8. Effects of extent of reduction on activity. (◇) 4.5% Fe/alumina (this study), (●) 1.8% Fe/alumina (*31*), (▼) 100% Fe (*67*), (◆) Fe/MgO (*7*), and (□) Fe/carbon (*9*).

supports dehydroxylated at 973 K or above, suggesting that the surface is free of support or oxide contaminants.

3. Fe/alumina CDCs prepared on highly dehydroxylated alumina are 2–10 times more active than CDCs prepared on poorly dehydroxylated alumina or than CPCs. This higher activity for the highly reduced catalysts can be attributed to their relatively clean metal surfaces while the lower activity of the poorly reduced CDCs and CPCs may be due to the presence on the metal surface of support or metal oxide contaminants.

4. Contrary to previous reports, the hydrocarbon product selectivity of CDCs prepared on highly dehydroxylated supports is typical of unpromoted iron catalysts and consistent with the Anderson–Schulz–Flory mechanism. The usually high selectivities for olefins reported earlier for CDCs are typical of those observed for poorly reduced Fe catalysts of low activity.

5. CO hydrogenation activity of Fe/alumina catalysts is better correlated with the extent of reduction than with dispersion. Accordingly, *CO hydrogenation on Fe/alumina is not structure-sensitive*, rather the observed changes in activity with dispersion are more likely a result of decoration of the metal surface by or strong interaction with support or metal oxide species.

APPENDIX A

Calculation of Percentage Dispersion and Percentage Reduction for Fe/Alumina CPC Assuming Fe(II) Is either Not Present or Is Not Oxidized during Titration

Experimental results
H_2 uptake (μmole) = 12.6
O_2 uptake (μmole) = 90.5
Fe loading = 4.05% = 725.2 μmole of Fe/g catalyst
Ratio of Fe^{3+}/Fe^{2+} areas (MES) = $\frac{1}{3}$

Reaction
$Fe^0 + (\frac{3}{4})\ O_2 \rightarrow (\frac{1}{2})\ Fe_2O_3$

Calculations

$$\% R = \frac{\mu\text{mole Fe metal } (10^2)}{\mu\text{mole total Fe in sample}} = \frac{\frac{4}{3}\,(\text{O}_2 \text{ uptake})\, 10^2}{725.2\ \mu\text{mole}}$$

$$= \frac{\frac{4}{3}\,(90.5)\, 10^2}{725.2} = 16.6$$

$$\% D = \frac{\text{number of surface Fe/metal atoms}}{\text{total number of Fe metal atoms}} = 1.117\ X/Wf$$

where X = H_2 uptake (μmole/g), W = wt% Fe, and f = fraction of iron reduced to metal (*9*).

$\% D = 1.117\ (12.6)/(4.05)\ (0.166) = 21$

APPENDIX B

CALCULATION OF PERCENTAGE DISPERSION AND PERCENTAGE REDUCTION FOR CONVENTIONAL FE/ALUMINA CATALYST (CPC) ASSUMING FE(II) IS PARTLY OXIDIZED DURING TITRATION

Reactions

$FeO + (\frac{1}{4})\, O_2 \rightarrow (\frac{1}{2})\, Fe_2O_3$ (1) (Oxidation of Fe^{II} to Fe^{III})

$Fe^0 + (\frac{3}{4})\, O_2 \rightarrow (\frac{1}{2})\, Fe_2O_3$ (2) (Oxidation of Fe^0 to Fe^{III})

Assumptions

1. Only $Fe^{(0)}$ adsorbs hydrogen (H/Fe = 1).
2. Fe^{2+} is present either as $FeAl_2O_4$ or as Fe_3O_4.
3. Fe^{3+} is only present in Fe_3O_4 ($[Fe^{2+}][2Fe^{3+}]\,O_4$), i.e., $Fe^{3+} : Fe^{2+} = 2:1$.
4. No Fe_2O_3 phase in the reduced catalyst.
5. Fe^{2+} in $FeAl_2O_4$ cannot be reduced or oxidized under these conditions.

Calculations

μmole of $Fe^{(0)}$ $= 725 \times 0.16 = 116$ (1st guess based on Mössbauer area)
μmole of iron oxide $= 725 - 116 = 609$
μmole of Fe^{3+} $= 609 \times (1/(1 + 3)) = 152$
μmole of Fe^{2+} in Fe_3O_4 $= 152 \times (\frac{1}{2}) = 76$

By Reaction (1)
Every mole of Fe^{2+} will need 0.25 mole of oxygen
76 μmole of Fe^{2+} will require $76 \times 0.25 = 19.0$ μmole of O_2

By Reaction (2)
Every mole of $Fe^{(0)}$ will need 0.75 mole of oxygen
116 μmole of $Fe^{(0)}$ will require $116 \times 0.75 = 87.0$ μmole of O_2

Total O_2 required = 19.0 + 87.0 = 106 μmole (calculated amount)
Experimentally 90.5 μmole of O_2.

Iterating with lower concentration of $Fe^{(0)}$ until experimental and calculated amounts are matched leads to the following results:
μmole of $Fe^{(0)}$ = 94.4
% dispersion $= [(12.5)\,(2) \times 100]/725(0.13) = 26.5$
% reduction $= (94.4 \times 100)/725 = 13.0$

ACKNOWLEDGMENTS

The authors gratefully acknowledge financial support by the Atlantic Richfield Co., Technology Coordination (later Corporate Technology) under the management of T. J. Clough and technical direction by J. W. Sibert and J. Labinger. The encouragement and technical assistance of P. Maxfield in preparation of the $Fe_3(CO)_{12}$ and of W. H. Lee, R. D. Jones, L. R. Neubauer, and P. A. Smith in the TPD and Mössbauer measurements is likewise acknowledged.

REFERENCES

1. Kelly, R. D., and Goodman, D. W., *Amer. Chem. Soc. Div. Fuel Chem. Prep. Pap.* **25**(2), 43 (1980).
2. Bartholomew, C. H., Pannell, R. B., and Butler, J. L., *J. Catal.* **65**, 335 (1980).
3. Kellner, C. S., and Bell, A. T., *J. Catal.* **75,** 251 (1982).
4. Boudart, M., and McDonald, M. A., *J. Phys. Chem.* **88**(11), 2195 (1984).
5. Reuel, R. C., and Bartholomew, C. H., *J. Catal.* **85,** 63 (1984).
6. Fu, L., and Bartholomew, C. H., *J. Catal.* **92**, 376 (1985).
7. MacDonald, M. A., Storm, D. A., and Boudart, M., *J. Catal.* **102,** 386 (1986).
8. Jung, H.-J., Walker, P. L., Jr., and Vannice, M. A., *J. Catal.* **75,** 416 (1982).
9. Jones, V. K., Neubauer, L. R., and Bartholomew, C. H., *J. Phys. Chem.* **90,** 4832 (1986).
10. Dwyer, D. J., and Somorjai, G. A., *J. Catal.* **52,** 291 (1978).
11. Johnson, B. G., Berlowitz, B. J., Goodman, D. W., and Bartholomew, C. H., paper in preparation, 1989.
12. Spencer, N. D., Schoonmaker, R. C., and Somorjai, G. A., *J. Catal.* **74,** 129 (1982).
13. Boudart, M., and Mariadassou, G. D., "Kinetics of Heterogeneous Catalytic Reactions," p. 154, Princeton Univ. Press, Princeton, NJ, 1984.
14. Eastman, D. E., Demuth, J. E., and Baker, J. M., *J. Vac. Sci. Technol.* **11,** 273 (1974).
15. (a) Erley, W., and Wagner, H., *Surf. Sci.* **74,** 333 (1978); (b) Erley, W., Ibach, H., Lehwald, S., and Wagner, H., *Surf. Sci.* **83,** 585 (1979).
16. Bridge, M. E., Comrie, C. M., and Lambert, R. M., *Surf. Sci.* **67,** 393 (1977).
17. Prior, K. A., Schwaha, K., and Lambert, R. M., *Surf. Sci.* **77,** 193 (1978).
18. (a) Papp, H., *Surf. Sci.* **129,** 205 (1983); (b) Papp, H., *Surf. Sci.* **149,** 460 (1985).
19. Kelley, R. D., and Goodman, D. W., *Surf. Sci.* **123,** L743 (1982).
20. Lee, D., Schmidt, L. D., Moulder, J. F., and Rusch, T. W., *J. Catal.* **99,** 472 (1986).
21. Kester, K. B., and Falconer, J. L., *J. Catal.* **89,** 380 (1984).
22. Kester, K. B., Zagli, E., and Falconer, J., *Appl. Catal.* **22,** 311 (1986).
23. (a) Huang, Y.-J., Schwarz, J. A., Diehl, J. R., and Baltrus, J. P., *Appl. Catal.* **36,** 163 (1988); (b) Huang, Y.-J., and Schwarz, J. A., *Appl. Catal.* **36,** 177 (1988).
24. Lee, W.-H., and Bartholomew, C. H., submitted for publication.
25. Raupp, G. B., and Dumesic, J. A., *J. Catal.* **95,** 587 (1985); **96,** 597 (1985); **97,** 85 (1986).
26. Bartholomew, C. H., *in* "Hydrogen in Catalysis" (Z. Paal and G. Menon, Eds.). Elsevier, Amsterdam, 1988.
27. Huang, Y.-J., Schwarz, J. A., Diehl, J. R., and Baltrus, J. P., *Appl. Catal.* **37,** 229 (1988).
28. (a) Brenner, A., and Hucul, D. A., *Inorg. Chem.* **18,** 2836 (1979); (b) Brenner, A., *J. Chem. Soc. Chem. Commun.*, 251 (1979); (c) Brenner, A., in "Metal Clusters" (M. Moskovits, Ed.), p. 249. Wiley, New York, 1986.
29. Phillips, J., and Dumesic, J. A., *Appl. Catal.* **9,** 1 (1984).
30. Zwart, J., and Snel, R., *J. Mol. Catal.* **30,** 305 (1985).
31. Rameswaran, M., Patil, M. D., Cable, T., and Bartholomew, C. H., in preparation, 1989.
32. McVicker, G. B., and Vannice, M. A., *J. Catal.* **63,** 25 (1980).
33. Chen, Y. W., Wang, H. T., and Goodwin, J. G., Jr., *J. Catal.* **83,** 415 (1983).
34. (a) Pannell, R. B., dissertation, Brigham Young University, 1977; (b) Bartholomew, C. H., and Pannell, R. B., *J. Catal.* **65,** 390 (1980).
35. Weatherbee, G. D., Rankin, J. L., and Bartholomew, C. H., *Appl. Catal.* **11,** 73 (1984).
36. Bartholomew, C. H., and Farrauto, *J. Catal.* **45,** 41 (1976).
37. Zowtiak, J. M., and Bartholomew, C. H., *J. Catal.* **83,** 107 (1983).
38. Lee, W.-H., Ph.D. dissertation, Brigham Young University, 1988.
39. Rameswaran, M., Ph.D. dissertation, Brigham Young University, 1986.
40. Bartholomew, C. H., "Investigation of Sulfur-Tolerant Catalyst for Selective Synthesis of Hydrocarbon Liquids From Coal-Derived Gases," Final Technical Progress Report to DOE, DOE-ET-14809-13, October 20, 1984.
41. Bhide, V. G., and Date, S. K., *Phys. Rev.* **172,** 345 (1968).
42. Yoshioka, T., Koezuka, J., and Ikoma, H., *J. Catal.* **16,** 264 (1970).
43. Garten, R. L., *J. Catal.* **43,** 18 (1976).
44. Lázár, K., Matusek, K., Mink, K., Dobos, S., Guczi, L., Vizi-Orsz, A., Markó, L., and Reiff, W. M., *J. Catal.* **87,** 163 (1984).
45. Jackson, R. L., and Trusheim, M. R., *J. Amer. Chem. Soc.* **104,** 6590 (1982).

46. Farmery, K., Kilner, M., Greatrex, R., and Greenwood, N. W., *J. Chem. Soc. A*, 2339 (1969).
47. Iwasawa, Y., Yamada, M., Ogasawara, S., Sato, Y., and Kuroda, M., *Chem. Lett.*, 621 (1983).
48. Vaishnava, P. P., Ktorides, P. I., Montano, P. A., Mbadcam, K. J., and Melson, G. A., *J. Catal.* **96,** 301 (1985).
49. Greenwood, N. N., and Gibb, T. C., "Mössbauer Spectroscopy," Chap. 10. Chapman & Hall, London, 1971.
50. Kündig, W., Bömmel, H., Constabaris, G., and Lindquist, R. H., *Phys. Rev.* **142,** 327 (1966).
51. Garten, R. L., and Ollis, D. F., *J. Catal.* **35,** 232 (1974).
52. Neubauer, L. R., Ph.D. dissertation, Brigham Young University, 1986.
53. Brenner, A., and Burwell, R. L., Jr., *J. Amer. Chem. Soc.* **97,** 2565 (1975).
54. Brenner, A., and Burwell, R. L., Jr., *J. Catal.* **52,** 353 (1978).
55. Hucul, D. A., and Brenner, A., *J. Amer. Chem. Soc.* **103,** 217 (1981).
56. Hucul, D. A., and Brenner, A., *J. Phys. Chem.* **85,** 496 (1981).
57. Wheeler, M. A., and Bettman, M., *J. Catal.* **40,** 124 (1974).
58. Bartholomew, C. H., *in* "Hydrogen in Catalysis" (Z. Paal, and G. Menon, Eds.), Chap. 5. Elsevier, Amsterdam, 1988.
59. Weatherbee, G. D., and Bartholomew, C. H., *J. Catal.* **87,** 55 (1984).
60. Le Caër, G., Dubois, J. M., Pijolat, M., Perrichon, V., and Bussiere, P., *J. Phys. Chem.* **86,** 4799 (1982).
61. Tau, L. M., Borcar, S., Bianchi, D., and Bennett, C. O., *J. Catal.* **87,** 36 (1984).
62. Vaishnava, P. P., Ktorides, P. I., Montano, P. A., Mbadcam, K. J., and Melson, G. A., *J. Catal.* **96,** 301 (1985).
63. Commereuc, D., Chauvin, Y., Hugues, F., Basset, J. M., and Olivier, D., *J. Chem. Soc. Chem. Commun.*, 154 (1980).
64. Hugues, F., Besson, B., and Basset, J. M., *J. Chem. Soc. Chem. Commun.*, 719 (1980).
65. Hugues, F., Bussiere, P., Basset, J. M., Commereuc, D., Chauvin, Y., Bonneviot, L., and Olivier, D., *Stud. Surf. Sci. Catal.* **7** (1981).
66. Kuznetsov, V. L., Danilyuk, A. F., Kolosova, I. E., and Yermakov, Y. I., *React. Kinet. Catal. Lett.* **21,** 249 (1982).
67. Bartholomew, C. H., and Rankin, J. L., in preparation, 1989.
68. Lee, W. H., and Bartholomew, C. H., in preparation, 1989.
69. Rankin, J. L., and Bartholomew, C. H., *J. Catal.* **100,** 526 (1986).
70. Anderson, R. B., "The Fischer–Tropsch Synthesis." Academic Press, New York, 1984.